

## Electronic structure and magnetism of $\text{EuTiO}_3$ : a first-principles study

This article has been downloaded from IOPscience. Please scroll down to see the full text article.

2007 J. Phys.: Condens. Matter 19 406217

(<http://iopscience.iop.org/0953-8984/19/40/406217>)

View [the table of contents for this issue](#), or go to the [journal homepage](#) for more

Download details:

IP Address: 129.252.86.83

The article was downloaded on 29/05/2010 at 06:09

Please note that [terms and conditions apply](#).

# Electronic structure and magnetism of $\text{EuTiO}_3$ : a first-principles study

Rajeev Ranjan<sup>1,2</sup>, Hasan Sadat Nabi<sup>2</sup> and Rossitza Pentcheva<sup>2</sup>

<sup>1</sup> School of Materials Science and Technology, Institute of Technology, Banaras Hindu University, Varanasi-221005, India

<sup>2</sup> Department für Geo- und Umweltwissenschaften, Sektion Kristallographie, Ludwig Maximilians Universität, Theresienstrasse 41, 80333 München, Germany

Received 13 July 2007, in final form 21 August 2007

Published 12 September 2007

Online at [stacks.iop.org/JPhysCM/19/406217](http://stacks.iop.org/JPhysCM/19/406217)

## Abstract

Density-functional theory calculations were carried out for the multiferroic  $\text{EuTiO}_3$  using the LDA +  $U$  approach. Total-energy calculations for ferromagnetic (F), and antiferromagnetic A-, C-, and G-type arrangements in the cubic phase shows that the ground-state magnetic configuration is G-type antiferromagnetic for  $U \leq 6$  eV and ferromagnetic for  $U \geq 7$  eV. Values of first- and second-neighbour exchange integrals have been calculated by mapping the energy difference between the different magnetic configurations to a Heisenberg Hamiltonian. The system seems to be critically balanced between ferromagnetic and antiferromagnetic states for realistic values of  $U$ , and switches from antiferromagnetic to a ferromagnetic ground state on hydrostatic expansion of volume.

## 1. Introduction

$\text{EuTiO}_3$  (ETO), like  $\text{SrTiO}_3$  (STO),  $\text{KTaO}_3$  (KTO) and  $\text{BaZrO}_3$  (BZO), is one of the rare perovskites that exhibits cubic symmetry (space group  $Pm\bar{3}m$ ) at ambient conditions [1–3]. However, unlike the other cubic perovskites, mentioned above, ETO exhibits magnetic ordering below 5.5 K [4–6]. The dielectric permittivity of ETO also exhibits an anomaly at the magnetic ordering temperature [4], suggesting magnetoelectric coupling of the polarization and magnetization. However, compared to other well-known magnetoelectrics [7–9], ETO has been less investigated. Very recently, using first-principles technique, a design strategy for magnetic and electric phase control in epitaxial ETO has been proposed [10]. Although magnetic susceptibility measurements on ETO show features of antiferromagnetic ordering, the details of magnetic ordering have not been investigated in detail, presumably due to the fact that naturally occurring Eu has a very large absorption cross section for thermal neutrons. An old report, however, suggests a G-type antiferromagnetic (AFM) spin arrangement in ETO [5]. Magnetic susceptibility measurements have shown that ETO is one of the few antiferromagnetic materials with a positive Curie–Weiss constant ( $\theta = +3.8$  K) [5]. Since the magnetic ion,

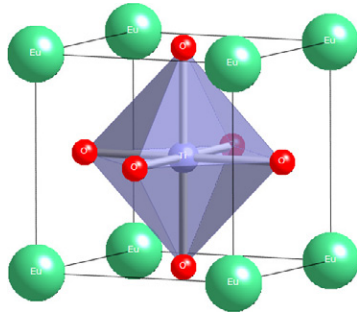


**Figure 1.** Crystal structure of cubic  $\text{EuTiO}_3$ . The corner atoms represent Eu, and the atoms at the body-centred and the face-centred positions represent Ti and O, respectively.

(This figure is in colour only in the electronic version)

$\text{Eu}^{2+}$ , in ETO occupies the A-site of the cubic perovskite structure (see figure 1), the nearest-neighbour (nn)  $\text{Eu}^{2+}$  magnetic ions see each other directly. On the other hand, the  $\text{O}^{2-}$  ions intercept in between the next-nearest-neighbour (nnn)  $\text{Eu}^{2+}$  ions. The  $\text{Eu}^{2+}$  valency results in a half-filled 4f shell. However, due to the localized nature of the f electrons, the exchange interaction between the nn and nnn  $\text{Eu}^{2+}$  ions is only possible through mediation of the other valence electronic states. A small intra-atomic admixture of 5d wavefunctions to the 4f states has been suggested in the past [6] as a possible mechanism of exchange in Eu compounds. With advances in *ab initio* electronic structure calculations based on density-functional theory (DFT), it has become possible to explain the electronic and magnetic properties of transition metal and rare earth compounds in significant detail. In this paper we report the results of DFT calculations for ETO using an all-electron approach and taking into account electronic correlations in the LSDA +  $U$  method. The magnetic ground state of this material is found to be dependent on the  $U$  parameter. The system seems to be critically balanced between antiferromagnetic (G-type) and ferromagnetic states for realistic values of  $U$ , and switchover from one state to another is possible by tuning the volume.

## 2. Computational details

Density-functional theory calculations were performed using the all-electron full-potential linearized augmented-plane-wave (FP-LAPW) method as implemented in the WIEN2k code [11]. The LAPW method is among the most accurate band structure methods currently available. The exchange–correlation potential is approximated by the generalized-gradient approximation (GGA) of Perdew *et al* [12]. The maximum  $l$ -value in the radial sphere expansion of the wavefunction was  $l_{\text{max}} = 10$ , and the largest  $l$ -value for the non-spherical part of potential and density was  $l_{\text{max,ns}} = 6$ . The cut-off energy,  $K_{\text{max}}^2$ , was fixed at 19 Ryd for the plane waves and  $G_{\text{max}} = 14$  for the charge density, so that no shape approximation to the potential occurs. The muffin-tin radii for Eu, Ti and O were chosen as 2.5, 1.9 and 1.6 au, respectively. We have used 30  $k$ -points in the irreducible part of the Brillouin zone (IBZ). Increasing the number of  $k$ -points to 140 in the IBZ led to changes in total energy smaller than 0.01–0.02 mRyd. In view of the small energy difference between the various magnetic configurations, the total energy was calculated with an accuracy of 0.02 mRyd.

A Hubbard-type on-site Coulomb repulsion parameter  $U$  was used to account for the strong correlations of the f electrons of Eu, as well as to ensure an insulating behaviour of this

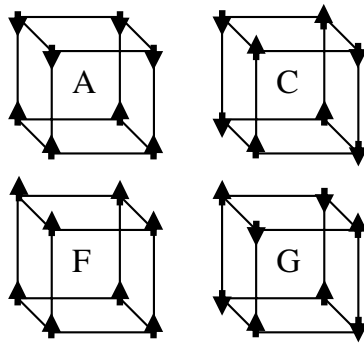


**Figure 2.** Schematic diagram of the four collinear magnetic structures, A, C, F, and G, considered for cubic  $\text{EuTiO}_3$ . The arrows indicate spin directions at the Eu sublattice.

compound in the band structure calculations [13]. Although the standard parameterization of the on-site Coulomb interaction involves two parameters,  $U$  and  $J$ , the completely filled spin-up  $f$  shell and completely empty spin-down  $f$  shell reduce the role of  $J$  to merely normalize the  $U$  value. We can, therefore, set  $J = 0$  and make use of an effective  $U$  in the calculations. Recent reports of DFT calculations on some europium compounds have validated the use of this approach for divalent Eu compounds as well [14–18].

### 3. Results and discussion

#### 3.1. Equilibrium lattice constant and bulk modulus

Since the structure of ETO has been reported to be cubic ( $Pm3m$ ) down to the lowest temperature, the only variable structural parameter is the lattice parameter,  $a_c$ . In general, for cubic perovskites, different magnetically ordered structures are possible [19, 20]. Total-energy calculations for four different collinear magnetic structures, A, C, F, and G, were considered in the present study. Of these, F corresponds to the ferromagnetic structure, while the other three correspond to different antiferromagnetic spin arrangements. A schematic diagram of the four magnetic structures is shown in figure 2. For the A-type antiferromagnetic structure, the nearest-neighbour moments are ferromagnetically coupled within a defined plane, and antiferromagnetically coupled between neighbouring planes. The reverse situation occurs for a C-type antiferromagnetic structure. For a G-type antiferromagnetic structure, all the nearest-neighbour moments are antiferromagnetically coupled. For the sake of technical consistency and to minimize the numerical error, we have chosen a tetragonal unit cell with four formula units of ETO for all the four magnetic structures considered above. The lattice parameters of the tetragonal cell ( $a_t$  and  $c_t$ ) are related to  $a_c$  in the following manner:  $a_t = \sqrt{2}a_c$ ,  $c_t = 2a_c$ . Total-energy versus volume calculations were performed to determine the equilibrium cell volume at  $U = 0, 3, 6$  and  $9$  eV. Figure 3 shows  $E(V)$  for  $U = 6$  eV. The energy differences between the various magnetic configurations are very small, and on the scale shown in this figure, the energies of the four magnetic configurations at any particular volume appear nearly degenerate. The theoretical equilibrium volume ( $\sim 246.6 \text{ \AA}^3$ ) is nearly insensitive to the different magnetic structures and also to the value of the  $U$  parameter used. The equivalent cubic lattice parameter,  $a = (V/4)^{1/3} = 3.950 \text{ \AA}$ , is larger than the experimentally reported value of  $3.905 \text{ \AA}$  [4] by 1%.

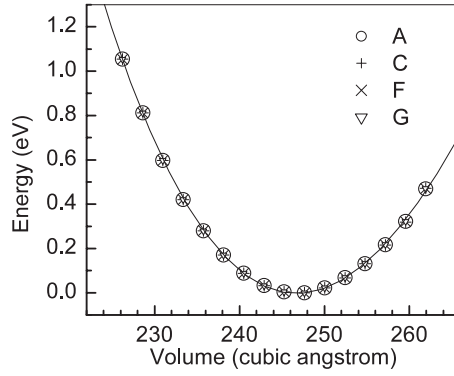


**Figure 3.** Total energy versus volume for F, A, C, and G magnetic structures of cubic  $\text{EuTiO}_3$  calculated at  $U = 6$  eV. The volume of the true cubic cell is four times smaller.

**Table 1.** Relative total energies of four different magnetic configurations of  $\text{EuTiO}_3$  at different values of  $U$ , calculated at the experimental lattice parameter. For each  $U$ , the lowest energy has been set to zero.

Magnetic configuration	Relative total energy (meV)						
	$U = 0$ eV	$U = 3$ eV	$U = 5$ eV	$U = 6$ eV	$U = 7$ eV	$U = 8$ eV	$U = 9$ eV
F	8.4	18.1	5.5	0.9	0.0	0.0	0.0
A	22.7	17.6	8.9	4.3	3.6	3.5	3.1
C	30.8	20.9	11.5	5.9	5.0	4.3	3.6
G	0.0	0.0	0.0	0.0	2.0	3.4	3.8

The value of the bulk modulus,  $B_0$ , and its pressure derivative  $B'_0$ , were obtained by fitting the Murnaghan equation of state [21, 22]:

$$E(V) = E_0 + \frac{B_0 V}{B'_0} \left( \frac{(V_0/V)^{B'_0}}{B'_0 - 1} + 1 \right) - \frac{B_0 V_0}{B'_0 - 1} \quad (1)$$

to the calculated  $E-V$  curve.  $B_0$  and  $B'_0$  were found to be 172.6 GPa and 4.1, respectively for  $U = 6$  eV. Since corresponding values from experiments are lacking, it was not possible to compare these numbers with corresponding experimental values for this material.

### 3.2. Electronic and magnetic structures of $\text{EuTiO}_3$

The total energy and total density of states (DOS) were calculated for the four magnetic configurations, F, A, C, and G, at the experimental lattice constant for  $U = 0, 3, 5, 6, 7, 8,$  and  $9$  eV. Table 1 lists the relative energies of the different configurations for each value of  $U$ . The lowest energy is assigned the value zero as reference energy. It is found that the G-type AFM structure possesses lowest energy for  $U \leq 6$  eV. For  $U \geq 7$  eV, the ferromagnetic (F) structure becomes stable (see table 1). Previous theoretical studies on divalent Eu compounds have reported that realistic values of  $U$  for Eu lie in the range  $6 \leq U \leq 9$  eV [16, 17]. Interestingly enough, we found that, at  $U = 6$  eV, the ground-state magnetic configuration changes from G-type AFM to ferromagnetic (F) on increasing the volume hydrostatically beyond the experimental value. Figure 4 shows the DOS plots for the F-, A-, C-, and G-type magnetic structures for  $U = 6$  eV. The essential features of the DOS plots for all the

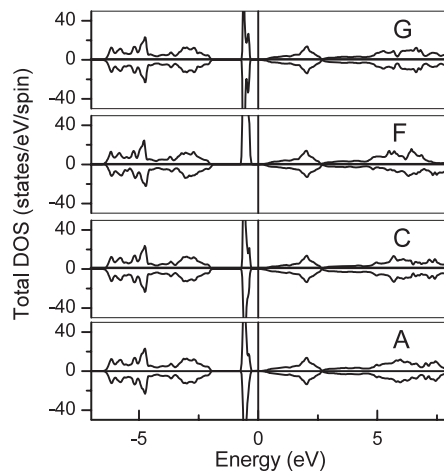


**Figure 4.** Total density of states for A, C, F, and G magnetic structures of  $\text{EuTiO}_3$  with  $U = 6$  eV.

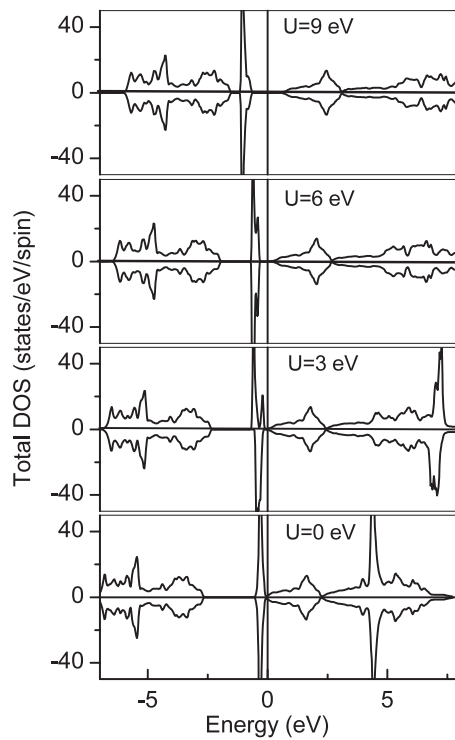


**Figure 5.** Total density of states for different values of  $U$  for the G-type magnetic structure of  $\text{EuTiO}_3$ .

configurations appear similar. Figure 5 shows representative DOS plots for the G-type AFM structure calculated at different  $U$  values. It is interesting to note that, compared to the occupied lower Hubbard  $f$  band, the unoccupied upper Hubbard  $f$  band shifts quite drastically with increasing  $U$ . For  $U = 0$  and 3 eV, the Fermi energy lies near the edge of the Ti 3d band,

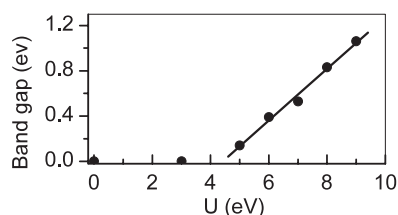


**Figure 6.** Variation of band gap of  $\text{EuTiO}_3$  with  $U$ .

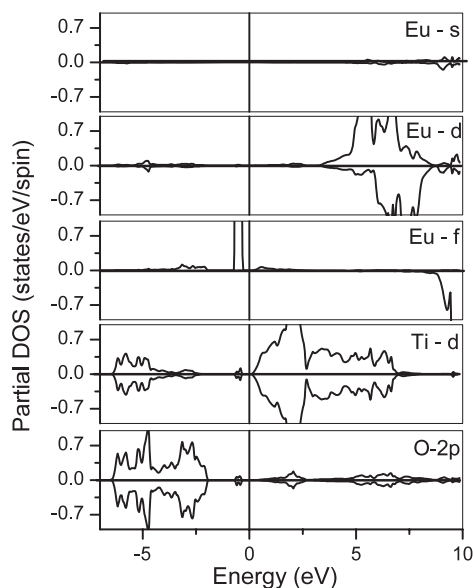


**Figure 7.** Partial density of states of Eu s, Eu d, Eu f, Ti d, and O p orbitals for the G-type magnetic structure ( $U = 6$  eV).

resulting in a metallic behaviour. A gap opens up for  $U \geq 5$  eV. Figure 6 shows the variation of band gap with  $U$ . The band gap increases from 0.14 eV at  $U = 5$ –1.1 eV for  $U = 9$  eV. A band structure plot revealed that the minimum of the band gap corresponds to the  $\Gamma$  point. The filled f band just below the Fermi level was nearly dispersionless. The maximum value of the gap (2.1 eV for  $U = 6$  eV) occurs at the R and X points of the cubic Brillouin zone.

Figure 7 shows the partial density of states (PDOS) for the O p states, Eu f and d states, and Ti d states in both spin channels. It is evident from this figure that the major contribution to the filled valence band comes from the O 2p states. A narrow occupied 4f band lies just below the Fermi level. A similar feature was also reported in the band structure of  $\text{EuS}$  [14]. The conduction band is formed by the Ti 3d states on the low-energy side and by the Eu 5d states at higher energies. Some fraction of the Ti d states is also occupied, suggesting some covalent bonding between the Ti and the O atoms, a feature common to most of the oxide perovskites. The absence of the Eu s states in the valence band part of the DOS suggests that Eu is almost completely ionized and forms ionic bonds with the O in the structure.

**Table 2.** Values of the first-nearest-neighbour ( $J_{ij}^{\text{nn}}$ ) and second-nearest-neighbour ( $J_{ij}^{\text{nnn}}$ ) exchange integrals (in units of kelvin) obtained after mapping the difference in the total energies of the various configurations, mentioned above, to a Heisenberg Hamiltonian (see text).

Exchange integral	$U = 0$ eV	$U = 3$ eV	$U = 5$ eV	$U = 6$ eV	$U = 7$ eV	$U = 8$ eV	$U = 9$ eV
$J_{ij}^{\text{nn}}$ (K)	-0.12	-0.24	-0.06	0.01	0.03	0.05	0.06
$J_{ij}^{\text{nnn}}$ (K)	0.26	0.12	0.08	0.05	0.04	0.03	0.02

### 3.3. Estimation of exchange integrals

We have calculated the nearest-neighbour (nn) and next-nearest-neighbour (nnn) exchange interactions ( $J_{ij}^{\text{nn}}$  and  $J_{ij}^{\text{nnn}}$ ) by mapping the energy difference between the different magnetic configurations of this system to the Heisenberg Hamiltonian as [23]

$$H = -2 \sum_{i>j}^N J_{ij} S_i \cdot S_j. \quad (2)$$

The ground state of  $\text{Eu}^{2+}$  ion corresponds to spin  $S = 7/2$  and orbital moment  $L = 0$ . The zero orbital moment adds a simplification to the calculations in the sense that the exchange interaction can be treated isotropic to a good approximation. The total numbers of nn and nnn  $\text{Eu}^{2+}$  bonds in the tetragonal cell considered for calculating the total energies are 12 and 20 respectively. The corresponding energy expressions for the four magnetic configurations, F, A, C, and G can be written as

$$E_F = E_0 + 2|S|^2(-12J_{ij}^{\text{nn}} - 24J_{ij}^{\text{nnn}}) \quad \text{for F type,} \quad (3)$$

$$E_A = E_0 + 2|S|^2(-4J_{ij}^{\text{nn}} + 8J_{ij}^{\text{nnn}}) \quad \text{for A type,} \quad (4)$$

$$E_C = E_0 + 2|S|^2(4J_{ij}^{\text{nn}} + 8J_{ij}^{\text{nnn}}) \quad \text{for C type,} \quad (5)$$

and

$$E_G = E_0 + 2|S|^2(12J_{ij}^{\text{nn}} - 24J_{ij}^{\text{nnn}}) \quad \text{for G type.} \quad (6)$$

Since  $S = 7/2$ ,  $|S|^2 = S(S + 1) = 15.5$  for  $\text{Eu}^{2+}$ . The values of the exchange interactions obtained with least squares fitting procedure, in units of kelvin, are listed in table 2. While  $J_{ij}^{\text{nn}}$  changes sign from negative to positive between  $U = 5$  and 6 eV, the sign of  $J_{ij}^{\text{nnn}}$  remains positive for all values of  $U$  under consideration. In general, it is noted that the value of  $J_{ij}^{\text{nn}}$  increases and that of  $J_{ij}^{\text{nnn}}$  decreases upon increase of  $U$ . Values of exchange integrals in ETO have also been reported in the past using parameters derived from temperature-dependent magnetic susceptibility measurements [5, 6]. The values of  $J_{ij}^{\text{nn}}$  and  $J_{ij}^{\text{nnn}}$  reported in [5] are  $-0.02$  and  $0.04$  K, respectively. Chien *et al* [6], on the other hand, have reported a slightly different value,  $J_{ij}^{\text{nn}} = -0.014$  K and  $J_{ij}^{\text{nnn}} = 0.037$  K. It is evident from table 2 that a similar value of  $J_{ij}^{\text{nn}}$  can be obtained theoretically for a value of  $U$  somewhere in the range  $5 \leq U \leq 6$  eV. The small values of the exchange constants indicate a very weak interaction between the magnetic ions in ETO. For  $\text{EuO}$  ( $T_C = 69$  K), the values of  $J_{ij}^{\text{nn}}$  and  $J_{ij}^{\text{nnn}}$  have been reported to be  $0.72$  and  $0.22$  K, respectively [14]. As can be noted,  $J_{ij}^{\text{nn}}$  in  $\text{EuO}$  is nearly 35 times larger than in ETO. This difference can be attributed in part to the larger Eu–Eu bond distances in ETO compared to  $\text{EuO}$ , and also to the relative arrangement of the oxygen ions around the Eu. In ETO the first-nearest-neighbour and the second-nearest-neighbour Eu ions lie at  $3.91$  Å, and  $5.53$  Å, respectively, while in  $\text{EuO}$  they are at  $3.63$  Å and  $5.14$  Å [24]. The second important factor is the fact that there are 12 oxygen atoms surrounding each Eu ion in the ETO structure as compared to 6 in  $\text{EuO}$ . This would result in a stronger shielding of



the d-state-mediated direct exchange interactions between the Eu ions in ETO compared to EuO, thereby weakening the strength of the exchange interactions in the former compound. In addition, the increased number of 90° cation–anion–cation superexchange between nearest-neighbour Eu atoms may promote ferromagnetic order, leading to a small negative value of  $J_{ij}^{\text{nn}}$  in ETO.

### 3.4. Incipient magnetoelectricity and possibility of non-collinear magnetic structure

As noted above, the exchange interactions are very weak in ETO, and  $J_{ij}^{\text{nn}}$  even changes sign in the critical region of  $U$ . The system seems to be critically balanced between a ferromagnetic (F) state and a G-type antiferromagnetic state. Further, the fact that the system is known to exhibit a dielectric anomaly at the magnetic ordering temperature (5.5 K) suggests that ETO may be considered as an incipient magnetoelectric multiferroic material. In the normal magnetoelectric multiferroics such as  $\text{RMnO}_3$  (with  $R = \text{Tb, Gd}$ ) [7, 25],  $\text{RMn}_2\text{O}_5$  ( $R = \text{Y, Tb}$  etc) [26], and hexaferrite [27], the ferroelectric order preferentially develops in spiral or helicoidal magnetic structures. The inversion symmetry in spiral magnetic structures is intrinsically broken, and such systems are close to becoming ferroelectric. The magnetic spiral can influence the charge and lattice via Dzyaloshinskii's antisymmetric exchange [28] to produce a ferroelectric state [29]. Although no ferroelectric behaviour has been reported in ETO, the anomaly in the dielectric permittivity at 5.5 K is indicative of a tendency to develop such an order. Since the temperature concerned is quite low, the quantum-mechanical fluctuations of the lattice, as has been reported in  $\text{SrTiO}_3$  [30], can suppress the onset of a regular ferroelectric state. In view of these recent developments in the understanding of the magnetoelectric multiferroic materials, and also the small energy difference between the various magnetic configurations observed in our calculations, a possibility of a non-collinear magnetic configuration in ETO cannot be completely ruled out. It may be mentioned again that due to very large absorption cross section of naturally occurring Eu for thermal neutrons, it is not easy to determine the magnetic structure of Eu compounds by neutron diffraction experiments.

## 4. Summary

We have studied the electronic structure and magnetic properties of cubic  $\text{EuTiO}_3$  using density-functional theory + Hubbard  $U$  (LDA +  $U$ ). The lowest-energy state corresponds to a G-type antiferromagnetic structure for  $U \leq 6$  eV and a ferromagnetic (F) structure for  $U \geq 7$  eV. The values of the first- and second-nearest-neighbour exchange integrals have been calculated by mapping the energy difference between four different magnetic configurations onto a Heisenberg Hamiltonian. The system is critically balanced between ferromagnetic and antiferromagnetic states for realistic values of  $U$ . The system switches from G-type AFM to a ferromagnetic ground state on increasing volume, opening a possibility of tailoring its magnetic properties, and also perhaps the associated dielectric properties, by appropriate chemical substitutions at the Ti site of this material.

## Acknowledgments

RR is grateful to the Alexander von Humboldt foundation for the award of a Humboldt research fellowship during his stay in Germany. We thank Jan Kuneš for helpful discussions.

## References

- [1] Borous J, Fankuchen I and Banks E 1953 *Acta Crystallogr.* **6** 67
- [2] Shafer M W 1965 *J. Appl. Phys.* **36** 1145

- [3] Janes D L, Bodnar R E and Taylor A L 1978 *J. Appl. Phys.* **49** 1452
- [4] Katsufuji T and Takagi H 2001 *Phys. Rev. B* **64** 054415
- [5] McGuire T R, Shafer M W, Joenk R J, Alperin H A and Pickart S J 1966 *J. Appl. Phys.* **37** 981
- [6] Chien C-L, De Benedetti S and Barros F De S 1974 *Phys. Rev. B* **10** 3913
- [7] Kimura T, Goto T, Shintani H, Ishizaka K, Arima T and Tokura Y 2003 *Nature* **426** 55
- [8] Fiebig M 2005 *J. Phys. D: Appl. Phys.* **38** R123
- [9] Hill N A 2002 *Annu. Rev. Mater. Res.* **32** 1
- [10] Fennie C J and Rabe K M 2006 *Phys. Rev. Lett.* **97** 267602
- [11] Blaha P, Schwarz K, Madsen G K H, Kvasnicka D and Luitz J 2001 *WIEN 2k, An Augmented Plane Wave + Local Orbitals Program for Calculating Crystal Properties* Karlheinz Schwarz, Techn. Universität Wien, Wien (ISBN 3-9501031-1-2)
- [12] Perdew J P, Bruke K and Ernzerhof M 1996 *Phys. Rev. Lett.* **77** 3865
- [13] Anisimov V I, Solov'yev I V, Korotin M A, Czyzyk M T and Swatzky G A 1993 *Phys. Rev. B* **48** 16929
- [14] Larson P and Lambrecht W R L 2006 *J. Phys.: Condens. Matter* **18** 11333
- [15] Kuneš J and Pickett W E 2005 *Physica B* **359–361** 205
- [16] Kuneš J, Ku W and Pickett W E 2005 *J. Phys. Soc. Japan* **74** 1408 (Preprint cond-mat/0406229)
- [17] Kuneš J and Pickett W E 2004 *Phys. Rev. B* **69** 165111
- [18] Kuneš J and Laskowski R 2004 *Phys. Rev. B* **70** 174415
- [19] Søndenå R, Ravindran P, Stølen S, Grande T and Hanfland M 2006 *Phys. Rev. B* **74** 144102
- [20] Ravindran P, Kjekshus A, Fjellvåg H, Delin A and Eriksson O 2002 *Phys. Rev. B* **65** 064445
- [21] Murunaghan F D 1944 *Proc. Natl Acad. Sci. USA* **30** 244
- [22] Anderson O L 1995 *Equations of State of Solids for Geophysics and Ceramic Science* (New York: Oxford University Press)
- [23] Yosida K 1996 *Theory of Magnetism (Springer Series in Solid State Sciences vol 122)* (Berlin: Springer) chapter 6
- [24] McGuire T R and Shafer M W 1964 *J. Appl. Phys.* **35** 984
- [25] Kenzelman M, Harris A B, Jonas S, Broholm C, Schefer J, Kim S B, Zhang C L, Cheong S-W, Vajk O P and Lynn J W 2005 *Phys. Rev. Lett.* **95** 087206
- [26] Hur N *et al* 2004 *Nature* **429** 392
- [27] Kimura T, Lawes G and Ramirez A P 2005 *Phys. Rev. Lett.* **94** 137201
- [28] Segienko I E and Dagotto E 2005 Preprint cond-mat/0508075
- [29] Anderson P W and Blount E I 1965 *Phys. Rev. Lett.* **4** 217
- [30] Müller K A and Burkard H 1979 *Phys. Rev. B* **19** 3593